

SOLUTIONS TO END- OF-CHAPTER PROBLEMS

for
Well Logging for Earth Scientists

by
Darwin V. Ellis and Julian M. Singer

Published by Springer, P.O. Box 17,
3300 AA Dordrecht, The Netherlands

2007

Solution to Problems

Chapter 2: Introduction to Well Log Interpretation

- 2.1 47.6%
- 2.1.1 85.8%
- 2.1.2 grain size variations, overburden compaction, cementation, clay-plugging
- 2.2 80.3%
- 2.3 39%
- 2.4 –
- 2.5 2.8 ft or 1.15 ft into formation.
- 2.6 114.6 ft

Chapter 3: Basic Resistivity and Spontaneous Potential

- 3.1 –
- 3.1.1 less saline
- 3.1.2 greater
- 3.1.3 Both GR and SP indicate shale, so $\varphi_n > \varphi_d$
- 3.1.4 1) 9320 – 9362 ft where $R_{xo} \approx R_t$, and 2) 9363 – 9394ft where $R_{xo} > R_t$. Both probably have hydrocarbons because R_t has increased above that of lower zone. Possible reasons include, decrease in porosity, presence of hydrocarbons or a change in water resistivity.
- 3.1.5 Lower, since R_{xo}/R_t suggests invasion.
- 3.2 An exercise in using Chart SP-4. Interpolate between results obtained for charts with $R_{xo} = R_t$ and $R_{xo} = 5 R_t$ in row for $R_t/R_m = 5$ to obtain $E_{SP}/E_{SP_{corr}} = 0.675$. So $E_{SP_{corr}} = -33.33$ mV.
- 3.3 $R_w = 0.172$ ohm-m. Using the uncorrected value, $R_w = 0.245$ ohm-m.
- 3.4.1 Using relation between resistance and resistivity; 46.5 k-ohm.
- 3.4.2 24.2 k-ohm. See chart Gen-6 for handy approximation.
- 3.4.3 1.26 k-ohm
- 3.5 –
- 3.5.3 The resistivity changes by nearly a factor of two but the temperature only by 10°F, so the salinity must change.
- 3.6 Deviation below 200°F negligible, but ~50% at 350°F.

Chapter 4: Empiricism: The Cornerstone of Interpretation

- 4.1 –
- 4.2 –
- 4.3 1) For any value of S_w the core with the greater porosity should be less resistive

- 2) Curve separation can be predicted using Archie's relation at any S_w , but separation is not as predicted.
- 4.4
- 4.41 R_w for sea water = 0.23 ohm-m (chart Gen-9). Use formation factor $(1/(0.2)^2)$ to find $R_o = 5.75$ ohm-m, so resistance = 0.46 ohm.
- 4.4.2 Using lower limit of marble resistivity from Table 3.1; resistance = 4×10^6 ohm.
- 4.5
- 4.5.1 From log find $R_t = 0.2$ ohm-m, so $F = 12.5$. If $S_w = 0.9$, then $R_w = 0.013$ ohm-m
- 4.5.2 ~ 300 kppm.
- 4.6
- 4.6.1 Obtain $R_t \sim 4$ ohm-m from the log; implies $\phi = 8\%$. For $S_w = 50\%$, $m = 1.63$.
- 4.6.2 $\phi = 12.6\%$
- 4.7
- 4.7.1 13–16% depending on porosity.
- 4.7.2 –
- 4.8 –
- 4.8.1 At $\phi = 0.1$, $T = 10$. At $\phi = 0.2$, $T = 5$.
- 4.9 $R_h = 9.8$ ohm-m. $R_v = 450$ ohm-m. R_h is closer to R_{sh} while R_v is closer to R_{sd}
- 4.10 39.3° or only 5.7° above horizontal.

Chapter 5: Resistivity: Electrode Devices

- 5.1.1 From givens deduce $R_t = 1.11$ ohm-m and $R_{xo} = 22.22$ ohm-m. Then, from geometric factors: $R_{LLd} = 5.966$ ohm-m and $R_{LLd} = 10.19$ ohm-m
- 5.2
- 5.2.1 $\sim 1\%$
- 5.2.2 $R_w = 8$ ohm-m.
- 5.3 The separation between the curves indicates invasion below 12540 ft and above 12470 ft. Elsewhere it is indeterminate.
- 5.4 $R_t = 1.6$ ohm-m. (All corrections are small). S_w from logs is $> 100\%$. S_w with correct R_t is 50% .
- 5.5 Hint given with problem.
- 5.6 85 m.
- 5.7 269 m and 0.08 ohm.

Chapter 6: Other Electrode and Toroid Devices

- 6.1 –
- 6.2
- 6.2.1 78.6%
- 6.2.2 10% uncertainty in porosity – $> 10\%$ uncertainty in S_w ; 10% uncertainty in R_w or in R_t – $> 5\%$ uncertainty in S_w .

6.3

6.3.1 Taking R_{xo} to be 1 ohm-m yields $\phi = 23\%$.

6.3.2 –

6.3.3 If $\phi = 30\%$, then $S_{xo} \neq 1$, but 78%.

6.4

6.4.1

Interval	R_t , ohm-m	D_i , in.
1	0.21	100
2	Av 1.2	Indeterminate
3	2.55	20

6.4.2 $R_w = 0.019$ ohm-m.

6.5

Depth, ft	R_{xo}/R_t	Fluid	S_w	Comment
12550	2.86	Water	100%	
12450	5	Water	> 100%	Uncertain invasion effect
12400	1	Mainly residual oil	51%	
12200	0.34	Movable oil	26%	
11800	0.02	Movable oil	44%	

6.6 $S_w = 58\%$

6.7 In top panel of Fig. 6.12, $D_i = 21$ in. In bottom panel $D_i = 25$ in.

In the top panel at $J = 0.5$, the apparent resistivity from the ring $R_t = 0.55 \cdot R_t$ while in the bottom panel $R_t = 5.5 \cdot R_t$. Therefore the ring reads closer to R_t in the top panel (conductive invasion).

Chapter 7: Resistivity: Induction Devices

7.1

7.1.1 Note minimum at mid-bed.

7.1.2 Using Fig. 7.10 find that 25% of response from below bed and 25% above bed of 40 in. thickness. $R_a = 9.09$ ohm-m.

7.1.3 9.09 ohm-m as above, but closer to correct value for sand bed.

7.1.4 For case of $R_{shale} = 5$ ohm-m, max. reading for detection is 5.5 ohm-m. Find that central bed must contribute 18% of response which corresponds to ~ 10 in. thick bed

7.2 Use Eq. 6.7 and log data from water zone at 5306 ft to get $S_w \sim 52\%$.

7.2.1 Use chart Rcor-5 which is very sensitive to bed thickness. Charts are presented for values of shoulder bed resistivity, 1.7 ohm-m in this case, so interpolate. Find $R_t \sim 6.4$ ohm-m instead of 5.5 ohm-m. Then $S_w \sim 65\%$.

- 7.3 Assuming that the residual oil saturation (ROS) is the same after invasion as after water flooding, ROS would be 27%.
- 7.4

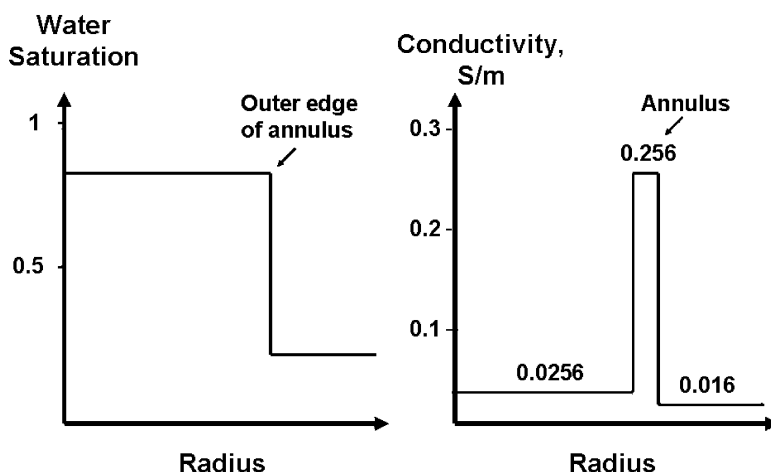
Interval	R_t , ohm-m	R_{xo} , ohm-m	Comment
A	1.8	10.8	In bottom half
B	11.7	129	
C	2.9	46	

The chart depends on R_{xo}/R_m because the radial response of ILd and ILM depends on resistivity level and is less at lower R_{xo} . The SFL reads less than R_{xo} by up to 35% because it sees beyond the invaded zone.

- 7.5 ILd should read closer at 30 ft, LLd at 120 ft. (Calculate R_{xo}/R_t and refer to Fig. 7-19.)
- 7.6 Using definition from Eq. 7.35 and noting that for $z > 0$ Eq. 7.33 can be written as $g(r,z) = (r^3)/(\rho^6)$, where $\rho^2 = z^2 + r^2$. Change variable of integration to $u = rmz^2 + r^2$ and integrate over appropriate limits.

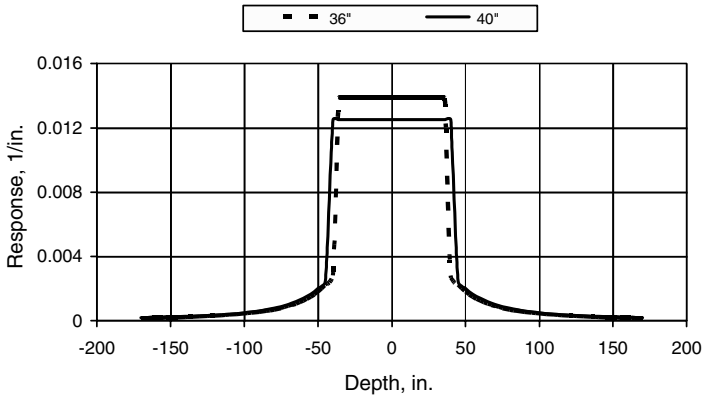
Chapter 8: Multi-Array and Triaxial Induction Devices

- 8.1 The error is 20% since R_t reads 0.4 ohm-m instead of 0.5 ohm-m. The error in S_w is 11% from Archie's equations.
- 8.2 The integrated vertical factor, G_{sh} , for the two shoulders is 0.00625.
- 8.2.1 The apparent resistivity in the center of the bed equals $G_{sh} * C_{sh} + (1 - G_{sh}) * C_t$, which gives 61.8 ohm-m.
- 8.3 From the D_i given in the figure and from Fig. 8-9, the integrated radial response of the 10 in. curve is 0.96 so that it should read 1.5 ohm-m.
- 8.3.1 When $R_t < R_f$.

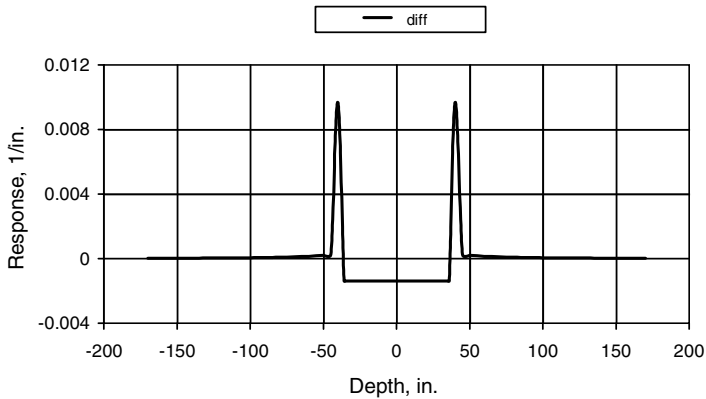


- 8.4 Radial profile of water saturation and conductivity with an annulus (above).
- 8.4.1 The maximum possible annulus thickness is 3.6 in. Calculate the volume of formation water originally in the flushed zone up to 48 in., and assume all this water goes into the annulus. Assume also that the original formation water in the annulus remains.
- 8.4.2 The conductivity is 0.055 S/m, which is higher than that in the flushed zone and the uninvaded zone.

Axial Response of 2 Two-Coil Arrays



Difference Between 2 Two-Coil Arrays



- 8.5 Vertical (axial) responses above.
- 8.6 There is an error in Eq. 8.6. in the text: k should be written as k_h . Then:

$$V = K \left[\frac{2i}{\omega \mu L^2} + \sigma_v - \sigma_v \frac{L}{\delta_h} (1 - i) - \sigma_v \frac{L \delta_v^2}{3 \delta_h^3} (1 - i) \dots \right]$$

- 8.6.1 6.9 S/m

8.7

Depth, ft	R _v , ohm-m	R _{sd} , ohm-m	V _{sh} , %
X420	1.1	2	49
X430	1.1	1.8	42
X440	1.8	2.5	30

$$8.7.1 \quad R_{sd} = \left[(R_v + R_h - 2V_{sh}R_h) + \sqrt{(R_v^2 - 2R_vR_h(1 - 2V_{sh} + 2V_{sh}^2) + R_h^2)} \right] / 2(1 - V_{sh})$$

R_{sh} can then be written out using Eq. 8.8.

Chapter 9: Propagation Measurements

- 9.1 Prove by direct comparison of the real and imaginary parts.
- 9.2 Write ε as $(\varepsilon' + i\varepsilon/\omega\varepsilon_0)$ from Eq. 9.10 and below, and ignore ε' .
- 9.3 At induction frequencies ε'' ranges from 10^3 to 10^7 , while ε' rarely reaches 10^3 . At laterolog frequencies ε'' ranges from 10^5 to 10^9 , while ε' rarely reaches 10^5 . (see Bona et al., reference 4)
- 9.4 $R_t = 40$ ohm-m, $\varepsilon' = 40$.
- 9.4.1 $R_{ps} = 39$ ohm-m, $R_{ad} = 40$ ohm-m from Fig. 9-14.
- 9.4.2 $R_{ps} = 40$ ohm-m, $R_{ad} = 40$ ohm-m.
- 9.5

$R_{xo} > R_t$	$R_{ad} > R_{ps}$	Resistive invasion, tool close to resistive boundary
$R_{xo} > R_t$	$R_{ad} < R_{ps}$	Resistive invasion
$R_{xo} < R_t$	$R_{ad} > R_{ps}$	Unlikely
$R_{xo} < R_t$	$R_{ad} < R_{ps}$	Unlikely
$R_{xo} = R_t$	$R_{ad} > R_{ps}$	Tool close to conductive boundary
$R_{xo} = R_t$	$R_{ad} > R_{ps}$	Large dielectric effects

- 9.5.1 With conductive mud, the uncorrected short-spaced measurements may read too low for both R_{ps} and R_{ad} . The table is still valid except that there could also be resistive invasion for the case of $R_{xo} > R_t$ and $R_{ad} < R_{ps}$. Oil-base mud can cause the long-spaced measurements of an eccentric tool to read higher than the short-spaced. The effect on the table is therefore similar to that of a conductive mud.
- 9.5.2 If the uncorrected short-spaced measurements read higher than the long-spaced, then the corrected measurements would read even higher and the same table remains valid.
- 9.6 Anisotropy. $R_{ps} > R_{ad}$, which could be resistive invasion except that the deeper readings read higher.

Chapter 10: Basic Nuclear Physics for Logging Applications: Gamma Rays

- 10.1 Hint: use Sterling's approximation.
10.2
10.2.1 $dN/N = -\mu x d\rho$
10.2.2 1 p.u. uncertainty corresponds to $\sim \Delta\rho = 0.0155 \text{ g/cm}^3$. Estimate μ from Fig. 10.8 for Al; $dN/N = 4.6\%$
10.2.3 475 cps
10.3 $N(\text{CsCl}) \sim 1.4 \times 10^{22}$; $\text{Vol} \sim 1.8 \times 10^{-3} \text{ cm}^3$.
10.4 –
10.5 –
10.6 –

Chapter 11: Gamma Ray Devices

- 11.1 A/N_o , where A is atomic weight of isotope and N_o is Avogadro's number.
11.2 Use Eq. 11.3 to compute particle flux from U, T, and K. Estimate μ from Fig. 10.8 and average gamma ray energy (1 MeV) to be $\sim 0.06 \text{ cm}^2/\text{g}$. Use Eq. 10.2 and known half-lives to compute partial count rates: K—20.4 cps; U—2.5 cps; Th—1.5 cps.
11.3

Depth, ft	Vcl(GR)	Vcl(SP)
8530	0	0
8549	50%	70%
8560	10%	50%

Thin bed at bottom?

- 11.4 $\sim 10\% \text{ \& } \sim 60\%$
11.5 Use only W_4 and W_5 to get two simultaneous equations:
 $W_4 = a_{41}Th + a_{42}U$
 $W_5 = a_{51}Th + a_{52}U$
after assuming that the K contributions a_{43} and a_{53} are zero.
11.6 Evaluate coefficients of prob. 11.5 using givens.

Chapter 12: Gamma Ray Scattering and Absorption Measurements

- 12.1 Find porosity $= 26.2\%$. Naïve hydrocarbon density $= 0.32 \text{ g/cm}^3$. Instead, compute electron density of hydrocarbon to be 0.48 g/cm^3 . Use data from Table 12.1 to find $\rho_b = 0.87\rho_e$ for CH_2 , so $\rho_{HC} = 0.42 \text{ g/cm}^3$.
12.1.1 $\rho_{log} = 1.07\rho_e - 0.1823$
12.2

- 12.2.1 Density varies between $2.30 - 2.37 \text{ g/cm}^3$. Formation might be limestone or dolomite so maximum spread of porosity is 21.1 p.u. to 31.2 p.u.
- 12.2.2 Cross plot density and P_e using chart CP-16 or Fig. 12.19 to find $\phi \sim 24 \text{ p.u.}$
- 12.2.3 From crossplot limestone fraction varies between 40% – 95%.
- 12.3
- 12.3.1 –
- 12.3.2 For salt-plugged formation, $\rho_b = 2.73 \text{ g/cm}^3$ & $P_e = 3.37$. Similar to a 5-6 p.u. water-filled limestone-dolomite mixture.
- 124 –
- 12.5.1 2.82 g/cm^3
- 12.5.2 0.08 v/v (8 p.u.)
- 12.5.3 7.7% pyrite
- 12.5.4 1.195 g/cm^3

Chapter 13: Basic Neutron Physics for Logging Applications

- 13.1
- 13.1.1 Note from conservation of momentum that He^4 velocity is $1/4$ neutron velocity. 14.08 MeV.
- 13.1.2 13.2 MeV.
- 13.2
- 13.2.1 Use data from Table 13.1 or Table 15.1, and Fig. 13.16. $\Sigma(\text{water}) = 22 \text{ cu}$, note that 10^{-3} times capture unit (cu) has dimension of cm^{-1} (it is the probability of being absorbed per cm). So Eq. 13.30 has proper units (4.5 cm).
- 13.2.2 4.2 cm for 0 p.u. and 3 cm for 20 p.u.
- 13.3 From data of Table 13.1 and weight fractions of H and Cl, contribution of H is 21 cu and Cl is 33 cu.
- 13.3.1 See Fig. 13.7
- 13.3.2 43.7 cu

Chapter 14: Neutron Porosity Devices

- 14.1
- 14.1.1 Epithermal tool responds to L_s , so use Fig 13.10 or Fig 14.14 to construct chart.
- 14.1.2 The correction is not a constant but a function of porosity as found above.
- 14.2
- 14.2.1 From Fig. 14.6 deduce a 7 p.u. shift from sand to limestone. Apparent limestone porosity $\sim 33 \text{ p.u.}$
- 14.2.2 Compute L_m (after computing Σ_{for} to be $\sim 53 \text{ cu}$ with inclusion of salt water); $\phi_{lime} \sim 55 \text{ p.u.}$

- 14.2.3 After recomputing apparent L_s and combining with the previously determined L_d , the L_m value yields an apparent porosity of 43 p.u.
- 14.3 See Fig. 14.14
- 14.4 33 p.u.
- 14.4.1 Using the data of Fig 14.12 (with a magnifying glass) or a chartbook, estimate that the temperature correction at 33 p.u. is on the order of 11 p.u., so ϕ_n will read 11 p.u. too low, showing cross-over at the two cleanest zones.
- 14.5 Using data from Reference 7 (Chapter 50) or estimating neutron response on the basis of hydrogen index, the cross-over is found to be ~ 6 -7 pu.
- 14.6 Hydrocarbon density, for one.
- 14.7 ~ 26 pu, see Section 21.3.2.

Chapter 15: Pulsed Neutron Devices and Spectroscopy

- 15.1 Solution density increases with addition of NaCl.
- 15.2 See Eq. 13.5
- 15.3 Use data of Table 13.1
- 15.4
- 15.4.1 Make a S vs ρ_b cross-plot using three end points:
 Water: 65 cu, 1.1 g/cm³
 Oil: ~ 21 cu, ~ 0.8 g/cm³
 Limestone: ~ 9 cu, 2.71 g/cm³
 Scale in S_w between water and oil points.
- 15.4.2 Find R_w @ 100°C. Then S_w from LLD is $\sim 48\%$. However, from Σ , S_w is $\sim 15\%$. Fresh water has diluted the formation water.
- 15.4.3 Iterate on values of salinity, computing S_w from Σ and LLD until values agree. Find salinity ~ 45 kppm and $S_w \sim 70\%$.
- 15.5 –
- 15.5.1 From hydrocarbon zone (not the low-density gas) estimate 12.6 cu.
- 15.5.2 Putting line from matrix point through the cloud of water points, find $\Sigma \sim 19$ cu. Deduce $\Sigma_w = 34$ cu.
- 15.6 From Fig. 3.5 or chart book find 0.18 ohm-m @ 115°F implies 30 kppm. From slope of Fig. 15.1 determine $\Sigma_w = 32.2$ cu.
- 15.6.1 No change. R_w gives consistent estimate.
- 15.6.2 Invasion must be shallow.
- 15.7 Use data from Table 13.1
- 15.7.1 See prob. 13.3.1
- 15.8 Insufficient data on the log. The value of Σ_{for} is necessary but we can assume a reasonable value. From log at depth X150, $\Sigma = 15$ cu, $\phi_g = 20$ pu of which $\phi_{oil} = 3$ pu. From defining equation: $\Sigma = 15 = 0.8 * \Sigma_{ma} + .03 * 21 + 0.17 * \Sigma_{mix}$, the maximum value of 13.2 cu can be determined for the matrix. If Σ_{ma} is assumed to be 5 cu, then show $\Sigma_{mix} = 61$ cu. If connate water volume is 2 pu then its salinity will be 140 kppm from Fig. 15.1.

Chapter 16: Nuclear Magnetic Logging

- 16.1 5580 Gauss
- 16.2 5000
- 16.3 —
- 16.4 Look at variation of η/T . From Prob 3.6, η varies as $\eta_o \exp(1825/T)$. Find that increase of T2 of water with increase in temperature is predicted by η/T when viscosity variation is taken into account. For change from 50–100°C, graph shows x2 increase and η/T predicts x2.5.
- 16.5 An exercise in applying Eq. 16.32 (and 16.31).
- 16.6
 - 16.6.1 22 time units
 - 16.6.2 $110 \times P_{down} = 11 \times P_{up}$ by substitution.
- 16.7 The position sought is for the same (but unspecified) resonant frequency for the two species.
- 16.8 Taking T1 to be proportional to correlation time leads to $T2 \propto a^2/bD$. Show that $D = kT/(6\pi \eta a)$ to confirm the use of η/T to scale the x-axis of Fig. 16.4.

Chapter 17: Introduction to Acoustic Logging

- 17.1
 - 17.1.1 37°, 17.4°
 - 17.1.2 Neglecting tool diameter, 2.37 ft.
- 17.2
 - 17.2.1 1.25 $\mu\text{sec}/\text{ft}$
 - 17.2.2 ~ 66.7 kHz.
 - 17.2.3 ~ 18 kHz.
- 17.3 for $\Delta t_{mud} > \Delta t_{for}$; ~ 3.9 ft.
- 17.4 304.8

Chapter 18: Acoustic Waves in Porous Rocks and Boreholes

- 18.1 —
- 18.2 Use compressibility $= -1/V(dV/dP)=1/K$. For each volume $-V_1 C dp = dV_1$, to arrive at: $K_t = [V_1/K_1 = V_2/K_2]^{-1}$.
- 18.3
 - 18.3.1 From Eq. 18.2 use $(k_c)^{-1} = \frac{S_w}{k_w} + \frac{1-S_w}{k_{oil}}$ and substitute into Eq. 18.21.
 - 18.3.2 Use relation $k = \rho(V_p^2 - 4/3V_s^2)$; determine k at two different saturations (and densities)
- 18.4 From $V_s^2 = 3/4V_c^2 - 3/4B/\rho$, see upper limit is for $\rho \rightarrow \infty$; 6.75 km/sec.
- 18.5

18.5.1 240 $\mu\text{s}/\text{ft}$.

18.5.2 Using Fig. 18.2, ~ 32 p.u.

18.5.3 Using $V_s = \sqrt{\frac{\mu}{\rho}}$, when density decreases V_s increases, so $V_{s_dry} > V_{s_brine}$. Expect $V_{s_dry}/V_{s_brine} = \sqrt{\frac{\rho_{brine}}{\rho_{air}}} = 1.06$

Chapter 19: Acoustic Logging Methods

19.1 Plot selected values of Δt vs ϕ_d for upper and lower zones using lithology identified from text.

19.2 Assume tube wave can be identified. V_{tube} (Eq. 18.20) can be rewritten in terms of V_{mud} , formation density, ρ , and mud density. Solve for ρ , and combine with V_p and V_s to get elastic constants.

19.3

19.3.1 Average $\Delta t \sim 100 \mu\text{s}/\text{ft}$, corresponds to ~ 33 pu for $V_{pma} = 18,000 \text{ ft}/\text{sec}$. Variation is from 95–105 $\mu\text{s}/\text{ft}$ corresponding to 29.5 – 36.5 pu.

19.3.2 Correlation between increase in resistivity and Δt increase.

19.3.3 The gas effect may be masked by invasion.

19.3.4 Hole size change inducing cycle skip(?).

19.3.5 Shale.

19.3.6 $\Delta t_{ma} = 45 \mu\text{s}/\text{ft}$, $\Delta t_{fl} = 218 \mu\text{s}/\text{ft}$

19.4 From plotting data on Fig. 18.12, find $\Delta t_{ma} = 49 \mu\text{s}/\text{ft}$, $\Delta t_{fl} = 218 \mu\text{s}/\text{ft}$. Middle and lower zones are consistent; upper is shale(?).

19.5 At 25 kHz, $\lambda = 0.48 \text{ ft}$, so depth of investigation is about one wavelength.

Chapter 20: High Angle and Horizontal Wells

20.1 Taking the transition from sand to shale as 42 ft, and using Fig. 20.2, the dip angle is 3.5° .

20.1.1 9.8° .

20.1.2 Looking downhole the shale is approaching from above.

20.2 See, for example, the website: www.scacompanies.com/publications/newsletters/archives/winter03.html

20.3 Taking the thickness of the sand as 100 ft MD, TVT = 6.47 ft and TST = 6.45 ft.

20.3.1 TVT = 11.73 ft, TST = 11.67 ft.

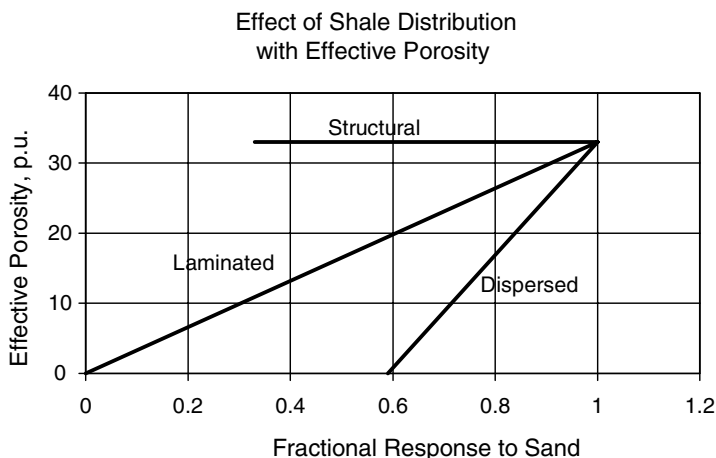
20.4 3 ohm-m. The induction tools.

20.5 88.6° .

20.6 The relative deviation is approximately 88.6° . The beds are thin enough that a density log perpendicular to them would read the average density, $2.25 \text{ g}/\text{cm}^3$.

Chapter 21: Clay Quantification

- 21.1 $150 \text{ cm}^2/\text{cm}^3$.
- 21.1 $6.9 \times 10^4 \text{ cm}^2/\text{cm}^3$.
- 21.3 2.52 g/cm^3 .
- 21.3.1 $Q_v = 0.02 \text{ meq per pore volume}$. $V_{cbw} = 0.2\%$.
- 21.4 –



- 21.4.1 Above, relationship between effective porosity and fractional sand volume.
- 21.4.2 Shale volume decreases with depth while total porosity also decreases, indicating structural shale.
- 21.5 Taking GR_{min} at 1870 ft = 19.5 gapi, and GR_{max} at 1665 ft = 96 gapi, then V_{sh} at 1700 ft = 5%. (Note: the clay weight % in Fig. 21.8 corresponds to GR_{min} at 1890 ft = 10 gapi, and GR_{max} at 1665 ft = 130 gapi, contrary to the numbers in the text.)
- 21.6 Expand the partial U_i contribution as $P_{e,i} \rho_{b,i}$. Divide both sides by density, ρ_b . Each terms is $P_{e,i}$ times weight fraction ($\rho_{b,i}/\rho_b$) and then use $P_{e,i} = (Z_i/10)^{3.6}$.
- 21.7 Calculate MW of kaolinite as ~ 231 . Weight fraction Al is 11.7% MW of illite ~ 254 . K weight fraction is 7.8%.
- 21.8 From the log the weight % of Al is $\sim 10\%$ and Fe wt% is 5%. Approximate MW of Illite (using Al) is ~ 700 . Reduce Al_5 to $\sim Al_{2.5}$. $Fe_{0.6}$ will produce $\sim 5\%$ Fe by weight.
- 21.8.1 Limestone from high P_e and low Al and GR.
- 21.9 $\sim 0.5\%$

Chapter 22: Lithology and Porosity Estimation

- 22.1 Should find (from top to bottom): Anhydrite, dolomite streak, mixed limestone-dolomite, a shale streak, mixed lime-dolomite, dolomite streak and finally limestone at 15380ft.

- 22.2 Assume ϕ_n in sandstone units, so first correct to limestone to use in cross plotting (correction can be done with charts like Fig. 21.1). Exercise in using Fig. 21.1 and Fig. 21.2. For computation of Δt_{ma} , use $\Delta t_f = 187 \mu\text{s}/\text{ft}$.
- 22.3 Compute P_e from U or short-cut of Eq. 21-13.
- 22.4 At e.g. 9900 ft, $\rho_{maa} = 2.71 \text{ g}/\text{cm}^3$ and $U_{maa} = 12$. The percentages of quartz, calcite and dolomite are 17%, 77% and 6%.
- 22.5 Density-sonic or density-neutron. For neutron-sonic the ~ 5 pu lithology shift could be masked by a Δt shift of only $4 \mu\text{s}/\text{ft}$.
- 22.6 Weight fraction of Ba in BaSO_4 is 58% so mud is 27% Ba by weight. $P_{e,mud} \sim 493 \times 0.27 = 133$. The mud is only 12% of formation density so $P_e \sim 19.9$.

Chapter 23: Saturation and Permeability Estimation

- 23.1 a. From the cross plot, $S_w = 100\%$ can be drawn through the uppermost points (7, 2, 11, 14, 9). For construction of graph can show $\sqrt{C_t} = \frac{S_w}{\sqrt{R_w}} \left(\frac{\Delta t - \Delta t_{ma}}{\Delta t_f - \Delta t_{ma}} \right)$. Assuming $\Delta t_f = 187 \mu\text{s}/\text{ft}$, take a conductivity point off 100% saturation line to compute $R_w = 0.085 \text{ ohm-m}$.
- b. From graphical inspection, $57 \mu\text{s}/\text{ft}$
- c. 16, 19, 3, 5, 6
- d. 29 p.u.
- 23.2 First compute porosity from Δt in previous problem, then plot $\log \phi$ vs $\log R_t$.
- a. Intercept at $\phi = 100$ gives $R_w \sim 0.88 \text{ ohm-m}$.
- b. From graphical inspection and Eq. 23.6, $m = \log(90)/\log(9) = 2.04$.
- c. From graphical inspection zone 3–40%; zone 14–50%, zone 17–50%, and zone 19–30%.
- 23.3 a) $F^* = 34.5$. b) $F = 18.5$.
- 23.4 $R_w = 0.017 \text{ ohm-m}$. C should produce oil (B has gas).
- 23.5 From Fig. 21-3 the total volume of water is $\phi_t S_{wt} = \phi_t - V_{hyd}$. Similarly the volume of effective water is $\phi_e S_{we} = \phi_e - V_{hyd}$ with V_{hyd} the same in both cases.
- 23.6 S_w with silt water is 48%, without silt water 25%. From Archie and R_h , $S_w = 49\%$.
- 23.6.1 $S_w = 44\%$. (Use Eq. 23.16 with silt instead of shale).
- 23.7 A reasonable approximation for $\log_{10} K$ in mD is $(17.1\phi_t - 2.29)$.
- 23.7.1 The Timur relation predicts much higher permeability than the correlation using ϕ_t . If ϕ_e is used the prediction is better, but still high.
- 23.8 $S_p = S_o \rho_{ma} (1 - \phi) / \phi$

Well Logging for Earth Scientists

Ellis, D.V.; Singer, J.M.

2007, XX, 708 p. 450 illus., Hardcover

ISBN: 978-1-4020-3738-2